

Conversion and temperature profiles during the photoinitiated polymerization of thick orthopaedic biomaterials

Jason A. Burdick, Alan J. Peterson, Kristi S. Anseth*

Department of Chemical Engineering, University of Colorado, Campus Box 424, Engineering Center, ECCH 111, Boulder, CO 80309-0424, USA

Received 2 August 2000; accepted 9 October 2000

Abstract

Polymerization of a tetrafunctional monomer was investigated under a variety of photoinitiation conditions to assess the ability to form thick materials in situ for orthopaedic applications. The major biological concerns include local cell and tissue necrosis due to the polymerization exotherm and low conversions at greater depths due to light attenuation through thick samples. Experimental results indicate that depth of cure and temperature rises are controllable by altering the photoinitiator concentration, initiating light intensity, and type of photoinitiator. For example, no measurable conversion was detected at a 1.0 cm depth when polymerization was initiated with 1.0 wt% DMPA and 100 mW/cm² ultraviolet light, whereas ~40% conversion was obtained when the initiator concentration was lowered to 0.1 wt%. This conversion was further increased to ~55% when a photobleaching initiator system was employed. At the highest rate of initiation studied (i.e., 1.0 wt% DMPA irradiated with 100 mW/cm² ultraviolet light), a maximum temperature of ~49°C was reached at the sample surface; however, this temperature dramatically decreased to ~33°C when the light intensity was decreased to 25 mW/cm². Finally, dual initiating systems that synergistically combine the advantages of photoinitiation and thermal initiation were investigated. © 2001 Elsevier Science Ltd. All rights reserved.

Keywords: Photopolymerization; Polyamides; Orthopaedic biomaterials; Temperature profile; Multifunctional monomers

1. Introduction

Typical surgical treatments for skeletal deficiencies (e.g. fractures, tumor removal) include the use of auto-grafts and allografts, metal fixation, ceramics, and bone cements [1]. There are problems associated with each of these techniques and materials. Grafts may be rejected by the body, induce cell morbidity and pain at the donor site, and are relatively costly. Nondegradable, metallic implants may loosen with time and require a second surgery for implant removal or replacement. Specifically, metal fixation devices are associated with stress shielding due to the high strength of the implant when compared to native bone and may corrode in the body. In recent years, degradable polymers have been investigated to replace these materials [2]. The flexibility in polymer design allows for a wide range of polymers with varying properties.

An additional advantage of polymeric biomaterials is the potential for in situ formation, which eliminates the need for ex situ implant fabrication and allows for the filling of irregular shaped bone defects. For example, methyl methacrylate is routinely polymerized in vivo to secure many orthopaedic prostheses. This polymerization occurs via thermal initiation at room temperature. However, numerous orthopaedic applications would benefit from in situ forming materials that are degradable. With this in mind, Mikos, Yaszemski, and collaborators [3,4] developed a class of degradable orthopaedic biomaterials based on polypropylene fumarate that were polymerized in situ using a thermal initiation system similar to PMMA bone cement.

In contrast to thermally initiated polymerization, photoinitiation can provide several advantages for orthopaedic applications. Photopolymerization allows for spatial and temporal control of the polymerization, allows rapid polymerization under physiological conditions, and is compatible for encapsulating certain drugs and growth factors that are subsequently released during degradation. In particular, our group has developed multifunctional anhydride monomers that can be

* Corresponding author. Tel.: + 1-303-492-7471; fax: + 1-303-492-4341.

E-mail address: kristi.anseth@colorado.edu (K.S. Anseth).

photocrosslinked in situ under clinical conditions [5] to yield highly crosslinked networks with enhanced mechanical properties when compared to linear polymers [6], controlled degradation rate and mechanism [6,7], and osteocompatibility [8].

Although the benefits of an in situ forming, photopolymerizable orthopaedic biomaterial are many, several potential disadvantages need to be considered and addressed. Photoinitiators are designed to absorb the initiating light and produce radicals; however, their absorption leads to light attenuation when polymerizing thick samples. Light attenuation decreases the rate of initiation, and subsequently the rate of polymerization, and conversions may be very low at appreciable depths in thick samples. Although multifunctional monomers gel at low conversions and give the system dimensional stability, potentially toxic monomer that is not crosslinked into the network can leach into surrounding tissues. Additionally, incomplete conversion (e.g., unreacted monomer or pendant double bonds) can dramatically decrease the mechanical properties of the polymers, which would be inappropriate for many load bearing orthopaedic situations.

A second major issue in developing an in situ polymerizing biomaterial is the temperature rise from the polymerization exotherm. This temperature rise may cause local cell morbidity and tissue necrosis surrounding the implant [9]. For instance, studies have been conducted on the temperature rise during polymerization of PMMA. In these thermally initiated polymerizations, reports have shown core temperatures that exceed 110°C and surface temperatures up to 60°C [10]. Since the initiation process is thermally triggered, exothermic temperature rises are exaggerated as the initiation rate dramatically increases with temperature.

An uncontrollable temperature rise can have a detrimental effect on the surrounding cells and tissue. For example, temperatures between 42 and 47°C are sufficient to kill many cell types [11]; proteins coagulate at 56°C; and bone collagen deteriorates at 70–72°C [12]. Additionally, cell death at the bone–implant interface can lead to the invasion of phagocytic cells and the production of a fibrous capsule. This capsule may allow for micromotion of the implant, resulting in small particles of cement settling in the tissue [13]. In addition, Chun et al. noted that periprosthetic osteolysis by phagocytic cells, including osteoclasts and macrophages, is associated with aseptic loosening and failure at the cement–bone interface [14]. Therefore, it is important to study the temperature rise during polymerization for better control during in situ polymerization.

The objective of this study was to characterize experimentally the temperature and conversion profiles during photopolymerization of thick polymer cylinders (up to 1.0 cm in thickness). Reaction parameters such as initiator concentration and light intensity were altered,

and their effects on these profiles were investigated for the polymerization of a tetrafunctional anhydride monomer. Photobleaching initiators, which lead to a self-eliminating light gradient upon irradiation, were also investigated. Finally, dual initiated systems containing both thermal and photoinitiators were studied to see if the depth of polymerization and final conversions could be enhanced.

2. Experimental

2.1. Materials

The multifunctional monomer used in these studies, methacrylated sebacic acid (MSA, Fig. 1), was synthesized as described elsewhere [5]. With addition of a photoinitiator and light, this dimethacrylated monomer radically polymerizes to form a highly crosslinked network. Photoinitiators used in this study include 2,2-dimethoxy-2-phenyl acetophenone (DMPA, Ciba-Geigy) and benzoin ethyl ether (BEE, Aldrich). DMPA is a common ultraviolet photoinitiator known for its high efficiency. BEE is another ultraviolet initiator, which has unique properties related to photobleaching. The amines and peroxides used in the dual initiating studies include *tert*-butyl peroxide (TBP), cumene hydroperoxide (CHP), triethylamine (TEA), and triethanolamine (TEOHA). These peroxide/amine systems were chosen based on their ability to initiate polymerization at temperatures slightly greater than room temperature. These chemicals were used as received from Aldrich.

Before polymerization, photoinitiators were dissolved in MSA at concentrations varying from 0.1 to 1.0 wt% at ~60°C and cooled to room temperature. If thermal initiators were used, the samples were prepared by dissolving the peroxide in the amine and mixing with MSA at room temperature. Polymerization was initiated with a Novacure (EFOS) light source with a 365 nm filter. Light intensities were adjusted by altering the distance of the light source from the sample. While these radical polymerizations are inhibited by the presence of oxygen, polymerizations were conducted under ambient conditions to simulate an in vivo environment.

Initiating conditions studied in this work include: 1.0 wt% DMPA and $I_0 = 100 \text{ mW/cm}^2$, 0.1 wt% DMPA and $I_0 = 100 \text{ mW/cm}^2$, 0.1 wt% DMPA and $I_0 =$

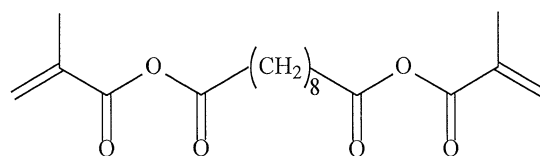


Fig. 1. Chemical structure of methacrylated sebacic acid (MSA).

25 mW/cm², 0.1 wt% BEE and $I_0 = 100$ mW/cm², and 1.0 wt% DMPA, 1.0 wt% peroxide/amine and $I_0 = 100$ mW/cm².

2.2. Methods

UV-Vis spectrophotometry (Model 8452, Hewlett Packard) was used to characterize the photobleaching of BEE with irradiation. BEE was dissolved in 1-hexanol, and the absorbance was measured after exposure to 100 mW/cm² ultraviolet light for 0, 1, 5, 10, and 15 min.

Conversion profiles were determined by real-time attenuated total reflectance Fourier transform infrared (ATR-FTIR) spectroscopy (Nicolet Magna-IR 750 Series II). Monomer samples of varying thickness (thin film to 1.0 cm) were polymerized directly on a ZnSe crystal (45° incidence angle) with exposure to ultraviolet light. While polymerizing, the area of the methacrylate peak (near 1637 nm⁻¹) was monitored in a thin layer adjacent to the ATR crystal. The conversion in this layer was calculated from the change in peak area as a function of polymerization time. The layer thickness (i.e., penetration depth of the evanescent wave) was calculated to be approximately 700 nm using the following formula [15]:

$$d_p = \frac{\lambda}{2\pi n_c [\sin^2 \Theta - (n_p/n_c)^2]^{1/2}} \quad (1)$$

Here, λ is the infrared wavelength being monitored, n_c is the refractive index of the ATR crystal, n_p is the refractive index of the polymer, and Θ is the angle of incidence of the internally reflected beam. One limitation of this technique for monitoring conversion is the fact that the refractive index of the sample changes with polymerization and can lead to changes in d_p . However, in quantifying our results, we did not observe that this was occurring to an appreciable extent. For example, when we examined a reference peak, such as the carbonyl, no changes were observed in the peak area during polymerization.

To monitor the temperature rise during polymerization, monomer/initiator samples were polymerized in a cylindrical Teflon mold. The mold dimensions were 1.0 cm in height and 1.0 cm in diameter, with thermocouples located at the surface and at depths of 0.5 and 1.0 cm.

3. Results and discussion

3.1. General polymerization behavior

The reaction behavior during the photoinitiated polymerization of a tetrafunctional monomer (MSA) that reacts to form a degradable network was investigated. These results address issues related to the suitability of

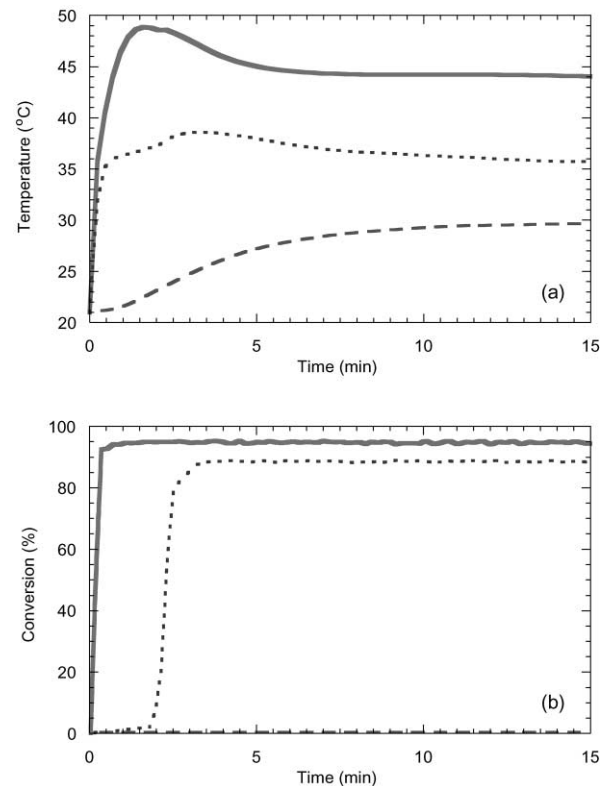


Fig. 2. Temperature (a) and conversion (b) profiles during the polymerization of MSA initiated with 1.0 wt% DMPA and 100 mW/cm² ultraviolet light; surface (solid line), 0.5 cm depth (dotted line), and 1.0 cm depth (dashed line).

photopolymerization for in situ forming highly cross-linked thick biomaterials, especially for orthopaedic applications. In particular, the conversion and temperature throughout a 1.0 cm thick sample was characterized under a variety of photoinitiation conditions. Initiation parameters that were investigated included the initiator concentration, irradiating light intensity, and type of photoinitiator.

The first system investigated was the photopolymerization of MSA with 1.0 wt% DMPA and 100 mW/cm² ultraviolet light. The temperature and conversion profiles during the polymerization of this system are shown in Fig. 2. The maximum temperature reached was ~49°C and occurred at the surface of the sample. At the surface, the temperature increased rapidly at early polymerization times, reached a maximum, and then leveled off at a temperature lower than the maximum. The temperature rise during the photopolymerization relates to both the exothermic nature of the polymerization and absorption of light by the sample during irradiation. Additionally, heat transfer throughout the sample and between the sample and the surroundings significantly affects the shape of the profile, so geometry of an in situ forming polymer can play an important role in the overall temperature profile (which was beyond the scope of this

study). The magnitude of the peak, as well as the time at which the maximum temperature occurred, decreased with sample depth and only reached $\sim 30^\circ\text{C}$ at a depth of 1.0 cm. This behavior couples strongly to the polymerization rate behavior discussed below. At a depth of 1.0 cm, where no conversion was measured, the temperature rise was attributed mainly to heat transfer from polymerizing regions in the sample.

FTIR data show that the rate of polymerization at the surface was very rapid with almost 95% conversion reached within 30 s. The shapes of the conversion curves show typical behavior for the photopolymerization of multifunctional monomers. There is an immediate onset of autoacceleration, since termination is diffusion controlled even at very low conversions. Eventually, propagation becomes diffusion controlled, and the system autodecelerates until a maximum conversion is reached. The maximum attainable conversion relates to limitations on the mobility of the reacting species and is coupled to the rate of polymerization through volume relaxation effects [16].

A lag in the polymerization rate occurs with depth and is attributed to oxygen inhibition. Oxygen acts as a radical scavenger and reacts with radicals to produce peroxy radicals with significantly lower reactivity [17]. However, once the dissolved oxygen was consumed, polymerization proceeds at a rate faster than the diffusion of oxygen through the polymerizing sample, and a conversion of $\sim 90\%$ was reached at a depth of 0.5 cm in less than 4 min. The difference in the final conversion between the surface layer and the polymer at 0.5 cm relates to the influence of volume relaxation. Rapidly polymerized systems can build up excess free volume, which leads to enhanced mobility and higher conversions compared to systems that are polymerized more slowly [16].

To better understand the differences in the conversion and temperature profiles as a function of depth during polymerization, a few of the governing equations are briefly reviewed. First, light attenuation as a function of sample depth is given by the Beer–Lambert Law:

$$I = I_0 \times 10^{-\varepsilon c_I z}. \quad (2)$$

Here, I is the light intensity at depth z , I_0 is the incident light intensity at the sample surface, ε is the molar absorptivity of the photoinitiator at the initiating wavelength, and c_I is the photoinitiator concentration. Utilizing this equation for DMPA (where ε is 1501/mol-cm at 365 nm), the light intensity at 1.0 cm was calculated to be approximately 0.3 mW/cm² compared to 100 mW/cm² at the surface. This significant decrease in the light intensity never leads to a rate of initiation that can overcome the effects of oxygen inhibition in the bottom layer of the sample. Additional factors, such as light scattering through the sample, may also contribute to further decreases in the light intensity at 1.0 cm.

As given in the following equation [18], the rate of initiation (R_i) is directly proportional to the light intensity:

$$R_i = 2\Phi f I, \quad (3)$$

where Φ is the quantum yield and f is the photoinitiator efficiency. Thus, the rate of initiation varies with position in the sample.

The overall polymerization rate is given by the following equation [18] for the consumption of double bonds with time:

$$-\frac{d[M]}{dt} = k_p[M] \left(\frac{R_i}{2k_t} \right)^{1/2}. \quad (4)$$

Here, $[M]$ is the concentration of double bonds, k_p is the propagation kinetic constant, k_t is the termination kinetic constant, and t is the polymerization time. As the polymerization proceeds, heat is generated ($Q \propto -d[M]/dt$), and a temperature rise occurs in the sample depending upon the relative rate of heat transfer to heat generation. In diffusion-controlled reactions, the kinetic constants change with both conversion and temperature. When the temperature begins to rise, the kinetics of the polymerization reaction will increase, which further increases the rate of heat generation, and can lead to thermal runaway. Because the rate of initiation is more dependent on temperature for a thermally initiated polymerization than a photoinitiated polymerization, thermal runaway is significantly more difficult to control with thermal initiation.

3.2. Changing the rate of initiation: initiator concentration effects

One approach to address problems associated with light attenuation is to decrease the initiator concentration. The overall shape of the temperature profiles (shown in Fig. 3(a)) did not change dramatically when the initiator concentration was lowered from 1.0 to 0.1 wt%. A slight decrease in the temperature rise is seen at all measured depths.

In contrast, dramatic changes are seen in the conversion profiles (shown in Fig. 3(b)) when the initiator concentration is decreased. The notable difference between the two systems is that almost 40% conversion is reached at 1.0 cm in the lower initiator concentration system, whereas no conversion was reached with the higher concentration. This demonstrates that reduced initiator concentrations absorb less of the irradiating light, thus allowing greater amounts of radiation to reach elevated depths. From Eq. (2), over 55 mW/cm² light reaches the 1.0 cm sample depth as compared to less than 1 mW/cm² when 1.0 wt% photoinitiator was used. Since the rate of initiation is directly proportional to the light intensity at each depth, decreasing the initiator concentration can

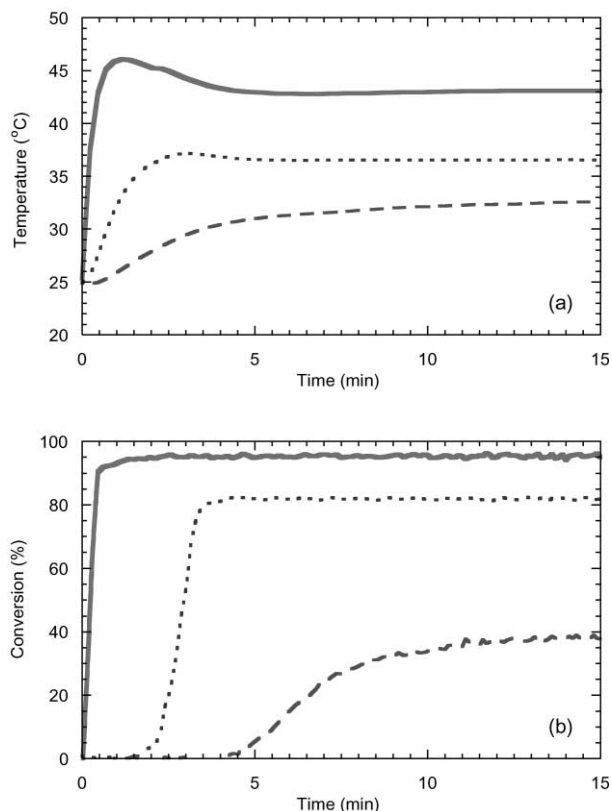


Fig. 3. Temperature (a) and conversion (b) profiles during the polymerization of MSA initiated with 0.1 wt% DMPA and 100 mW/cm² ultraviolet light; surface (solid line), 0.5 cm depth (dotted line), and 1.0 cm depth (dashed line).

significantly increase the polymerization rate at greater depths; however, the surface polymerization rate (where light attenuation is not a problem) will be decreased. The shapes of the curves are similar to Fig. 2 and exhibit all the classical features of diffusion-controlled crosslinking polymerizations. There is a slight increase in the lag time due to oxygen inhibition at the 0.5 cm sample depth. Additionally, the slope of the conversion curve is slightly less than before, indicating a lower rate of polymerization at both the surface and a depth of 0.5 cm. This is directly related to the decrease in the rate of initiation due to a decreased initiator concentration. For an in situ forming material, a balance exists between maintaining a reasonable overall rate of polymerization while providing the necessary depth of cure.

3.3. Changing the rate of initiation: light intensity effects

Although the conversion increased at depths of 0.5 and 1.0 cm when the initiator concentration was lowered, the polymerization still produces a relatively high temperature rise in the sample ($T_{\max} = 46\text{--}49^\circ\text{C}$). In general, the adiabatic temperature rise is fixed by the initial concentration of double bonds in the system and the final

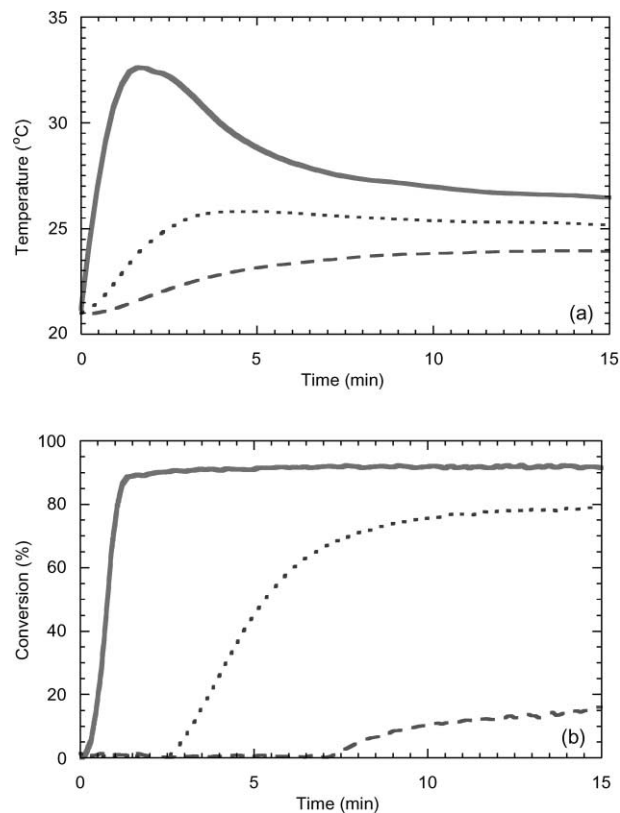


Fig. 4. Temperature (a) and conversion (b) profiles during the polymerization of MSA initiated with 0.1 wt% DMPA and 25 mW/cm² ultraviolet light; surface (solid line), 0.5 cm depth (dotted line), and 1.0 cm depth (dashed line).

conversion. However, when heat transfer is present, slowing the rate of polymerization allows one to control the rate of heat generation and more closely match the rate of heat transfer to minimize the temperature rise. To decrease the exothermic temperature rise during polymerization, the light intensity was decreased from 100 to 25 mW/cm² and used to initiate the 0.1% DMPA system. As shown in Fig. 4(a), this polymerization reached much lower temperatures than the same system irradiated at 100 mW/cm². The maximum temperature reached in this system was $\sim 33^\circ\text{C}$. This small temperature increase would be very appropriate for in situ curing biomaterials. The downfall to this approach for controlling the temperature rise is the increased polymerization time and the lower conversions with sample depth. As seen in Fig. 4(b), less than 20% conversion is reached at a depth of 1.0 cm. This low conversion results from the lower initiating intensity and the minimal temperature rise. From Eq. (2), the rate of initiation is directly proportional to the light intensity, and thus, the rate of initiation will be lower with a lower light intensity. Again, maximum conversion couples to volume relaxation effects, which are more pronounced at faster polymerization rates, and the kinetics of the polymerization are directly affected by

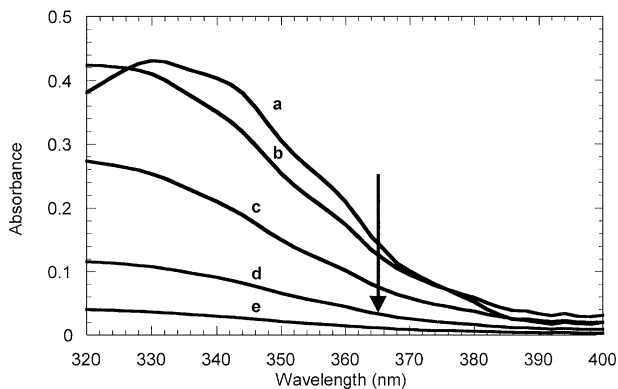


Fig. 5. Photobleaching of BEE during irradiation with 100 mW/cm^2 ultraviolet light. Arrow indicates increase in irradiation time from 0 (a), 1 (b), 5 (c), 10 (d), and 15 (e) min.

temperature. These factors synergistically combine to yield lower conversions at greater sample depths.

3.4. Light attenuation and photobleaching initiators

An alternative and promising approach to control the exothermic temperature rise and maintain appropriate polymerization rates with depth is the use of a photobleaching initiator. When a photobleaching initiator absorbs light and cleaves to form radicals, the photoproducts absorb at a wavelength different from the initiating wavelength, and thus, light can penetrate to greater depths with exposure time. The photobleaching of BEE was monitored using UV-Vis spectroscopy and is shown in Fig. 5. Since ϵ is proportional to the measured absorbance, these results indicate that the light intensity should increase by 20 and 32% after 5 and 10 min respectively, for a depth of 1.0 cm.

The temperature profile (shown in Fig. 6(a)) of the photobleaching initiator, BEE, is very similar to the temperature profile of the same system with DMPA as the initiator. The largest difference is the greater conversion that is obtained at a depth of 1.0 cm in the sample, $\sim 55\%$. Interestingly, the conversion at the 0.5 cm depth was greater than at the surface. One explanation for this result is the lower efficiency of BEE compared to DMPA. A lower efficiency would decrease R_p at the surface making it more difficult to overcome oxygen inhibition. Consistent with this explanation, there is a lag time at the surface for BEE, whereas with DMPA a lag time was not observed.

3.5. Dual initiation schemes

The addition of a thermal initiator to the above photo-initiating systems (dual initiation) provides synergistic advantages. First, polymerization begins at the surface of the sample (and everywhere the initiating light reaches)

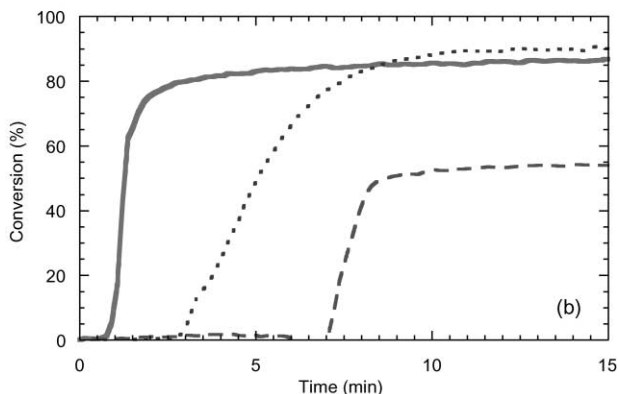
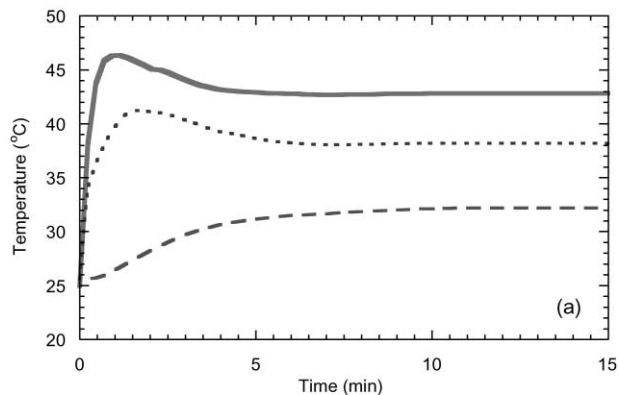


Fig. 6. Temperature (a) and conversion (b) profiles during the polymerization of MSA initiated with 0.1 wt% BEE and 100 mW/cm^2 ultraviolet light; surface (solid line), 0.5 cm depth (dotted line), and 1.0 cm depth (dashed line).

through photoinitiation. As the polymerization proceeds, heat is evolved which triggers the dissociation of the thermal initiators. In this manner, the two initiation mechanisms are coupled and occur on a similar time scale. Secondly, photopolymerization could be used to gel the system initially, while a much slower thermal initiated polymerization could subsequently increase the network conversion over a much longer time scale. For orthopaedic applications, the polymerization may need to reach crevices in a defect that light may not be able to penetrate. A benefit of a dual initiated system is that initiation from the heat generated in the exposed areas could give rise to radial cure and network formation in these dark areas. Scranton and collaborators have investigated this technique for the polymerization of thick composites for industrial applications [19].

In this study, both amine and peroxide initiators were chosen. The amine acts as an accelerator [18], which increases the decomposition rate of the system. Essentially, this initiation is a type of redox initiation. Redox initiation allows for a greater variety of initiation temperatures than is found with a direct thermal homolysis of

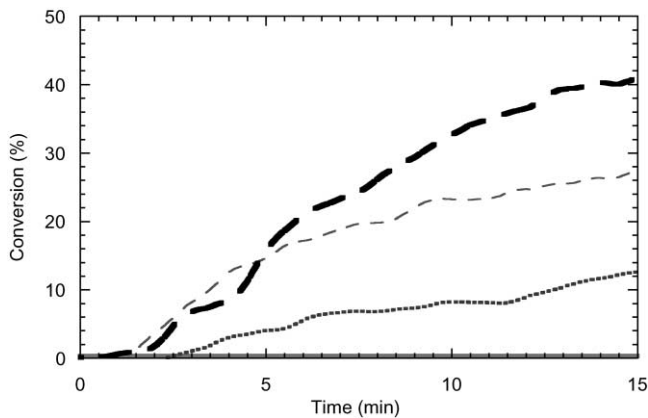


Fig. 7. Conversion profile during the polymerization of MSA initiated with 1.0 wt% DMPA and 100 mW/cm² ultraviolet light at a depth of 1.0 cm with addition of thermal initiators: no peroxide/amine (solid line), 1.0 wt% TEOHA/CHP (dotted line), 1.0 wt% TEOHA/TBP (thin dashed line), and 1.0 wt% TEA/TBP (thick dashed line).

only a peroxide. Additionally, this initiation is spatially uniform.

Thermal initiators were added during polymerization of MSA and 1.0 wt% DMPA with 100 mW/cm² ultraviolet light and the conversion was monitored at a depth of 1.0 cm. Recall that this system had no measurable conversion at 1.0 cm depth, and therefore, any increase in conversion would be attributable to the thermally initiated polymerization. For comparison, the thermal initiating systems were examined in a system with no DMPA and exposed to light at room temperature. No significant conversion was measured on the time scale of the experiment. Fig. 7 shows the conversion profile with the addition of these thermal initiating systems.

The solid line shows the lack of any polymerization in the system without a peroxide or amine present. Approximately 12% conversion was reached after 15 min with 1.0 wt% TEOHA/CHP. This level was increased to ~27% when the peroxide was changed to TBP, and to ~40% when the amine was changed to TEA.

An additional advantage of the peroxide/amine systems is the possibility of secondary polymerization on a much longer time scale. This property would be advantageous when using photopolymerization to quickly gel a network (i.e., fix the 3D shape), but the secondary polymerization would occur uniformly on a much longer time scale to insure complete conversion. This approach was investigated by curing a sample for 15 min, removing the light source, and monitoring the conversion after both 24 and 48 h. The results for the TEA/TBP system are shown in Fig. 8. After 24 h, an additional 15% conversion was obtained. After 48 h, an additional 5% cure was obtained, with a maximum of over 55% conversion.

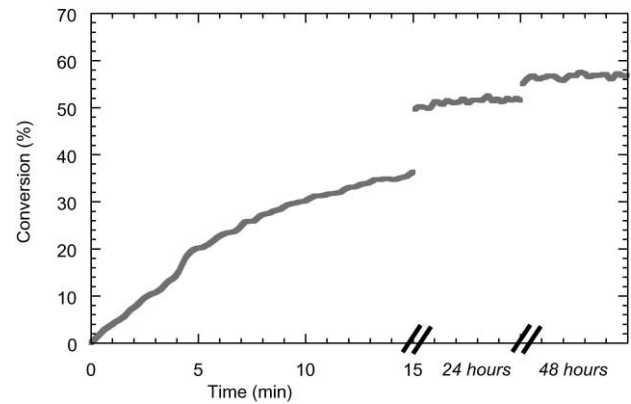


Fig. 8. Conversion profile during the polymerization of MSA initiated with 1.0 wt% DMPA, 1.0 wt% TEA/TBP, and 100 mW/cm² ultraviolet light at a depth of 1.0 cm for 15 min and then left to cure for 24 and 48 h.

4. Conclusions

The conversion and temperature profiles during photopolymerization of a dimethacrylated monomer were measured as a function of the rate of photoinitiation (i.e., changes in initiator concentration, light intensity, and type of photoinitiator). Decreasing the initiator concentration resulted in a slight decrease in temperature, but a significant increase in conversion at greater depths. A lower light intensity produced a much lower temperature rise, but also lower conversions. Finally, a photobleaching initiator was used to provide good depths of cure. Likewise, dual initiating systems of both thermal and photoinitiators have potential in situations where light is not able to penetrate the sample. These results indicate that the polymerizing system, with regard to temperature and conversion, is very controllable when compared to other in situ forming materials. Fewer problems, such as thermal runaway that may exist for PMMA bone cements, exist with photoinitiated in situ forming materials for orthopaedics.

Acknowledgements

The authors gratefully acknowledge funding from the National Science Foundation (BES-9734236), the National Institute of Health (AR44375-02), and a fellowship from the Colorado Institute for Research in Biotechnology for JAB.

References

- [1] Ishaug SL, Crane GM, Miller MJ, Yasko AW, Yaszemski MJ, Mikos AG. Bone formation by three-dimensional stromal osteoblast culture in biodegradable polymer scaffolds. *J Biomed Mater Res* 1997;36:17–28.

- [2] Behravesh E, Yasko AW, Engel PS, Mikos AG. Synthetic biodegradable polymers for orthopaedic applications. *Clin Orthop Relat Res* 1999;367S:S118–25.
- [3] Peter SJ, Nolley JA, Widmer MS, Merwin JE, Yaszemski MJ, Yasko AW, Engel PS, Mikos AG. In vitro degradation of a poly(propylene fumarate)/b-tricalcium phosphate composite orthopaedic scaffold. *Tissue Engng* 1995;1:41–52.
- [4] Peter SJ, Kim P, Yasko AW, Yaszemski MJ, Mikos AG. Cross-linking characteristics of an injectable poly(propylene fumarate)/v-tricalcium phosphate paste and mechanical properties of the crosslinked composite for use as a biodegradable bone cement. *J Biomed Mater Res* 1999;44:314–21.
- [5] Svaldi-Muggli D, Burkoth AK, Keyser SA, Lee HR, Anseth KS. Reaction behavior of biodegradable, photo-cross-linkable polyanhydrides. *Macromolecules* 1998;31:4120–5.
- [6] Svaldi-Muggli D, Burkoth AK, Anseth KS. Crosslinked polyanhydrides for use in orthopaedic applications: degradation behavior and mechanics. *J Biomed Mater Res* 1998;46:271–8.
- [7] Burkoth AK, Burdick J, Anseth KS. Surface and bulk modifications to photocrosslinked polyanhydrides to control degradation behavior. *J Biomed Mater Res* 2000;51:352–9.
- [8] Anseth KS, Shastri VR, Langer R. Photopolymerizable degradable polyanhydrides with osteocompatibility. *Nature Biotech* 1999;17:156–9.
- [9] Jefferis CD, Lee AJC, Ling RSM. Thermal aspects of self-curing poly(methyl methacrylate). *J Bone Jt Surg* 1975;57B:511–8.
- [10] Yamamuro T, Nakamura T, Iida H, Kawanabe K, Matsuda Y, Ido K, Tamura J, Senaha Y. Development of bioactive bone cement and its clinical applications. *Biomaterials* 1998;19:1479–82.
- [11] Lundskog J. Heat and bone tissue. *Scand J Plast Reconstr Surg* 1972;Supplement 9:1–80.
- [12] De Wijn JR, van Mullem PJ. Acrylics for implantation. In: Williams D, editor. *Concise encyclopedia of medical and dental materials*. Cambridge: The MIT Press, 1990. p. 14–21.
- [13] Anthony PP, Gie GA, Howie CR, Ling RSM. Localized endosteal bone lysis in relation to the femoral components of cemented total hip arthroplasties. *J Bone Jt Surg* 1990;72B:971–9.
- [14] Chun L, Yoon J, Song Y, Huie P, Regula D, Goodman S. The characterization of macrophages and osteoclasts in tissues harvested from revised total hip prostheses. *J Biomed Mater Res* 1999;48:899–903.
- [15] Harrick NJ. *Internal reflection spectroscopy*. New York: Wiley, 1967.
- [16] Anseth KS, Kline LM, Walker TA, Anderson KJ, Bowman CN. Reaction kinetics and volume relaxation during polymerizations of multiethylene glycol dimethacrylates. *Macromolecules* 1995;28:2491–9.
- [17] Decker C, Jenkins AD. Kinetic approach of O₂ inhibition in ultraviolet and laser induced polymerizations. *Macromolecules* 1985;18:1241–4.
- [18] Odian G. *Principles of polymerization*. New York: Wiley, 1991.
- [19] Narayanan V, Scranton AB. Photopolymerization of composites. *Trends Polym Sci* 1997;5:415–9.